

MALAYSIAN JOURNAL OF ANALYTICAL SCIENCES



Journal homepage: https://mjas.analis.com.my/

Research Article

Chitosan-microcrystalline cellulose aerogel films for methylene blue adsorption: A combined experimental and density functional theory study

Nur Aqilah Mokhtar¹, Nur Aida Fatimah Mashri¹, Noor Afizah Rosli^{1,3}, Najaa Mustaffa⁴, Suhaila Sapari⁴, Fazira Ilyana Abdul Razak⁴, Adhitya G. Saputro^{5,6}, and Nadhratun Naiim Mobarak^{1,2,3}

Received: 10 March 2025; Revised: 20 May 2025; Accepted: 25 May 2025; Published: 27 June 2025

Abstract

This study has investigated the effects of microcrystalline cellulose (C) on the swelling and adsorption characteristics of chitosan (CH)-based aerogels. The primary objective is to evaluate the impact of varying amounts of microcrystalline cellulose on the performance of chitosan-microcrystalline cellulose (CH-C) aerogels in methylene blue (MB) adsorption and swelling experiments. CH-C aerogel films were prepared by incorporating different quantities of microcrystalline cellulose into a chitosan solution, then freeze-dried. The results demonstrated that the addition of microcrystalline cellulose enhanced the strength of aerogel, allowing it to maintain its form when submerged in distilled water for 24 h. Although mechanical integrity improved with cellulose addition, the degree of swelling decreased due to stronger hydrogen bonding between chitosan and cellulose. Fourier transform infrared spectroscopy analysis indicated physical interactions between microcrystalline cellulose and chitosan. The adsorption process of MB on the CH-C aerogel revealed that it follows the pseudo-second-order kinetic model and the Langmuir isotherm model, suggesting that physical adsorption dominates this adsorption process. The adsorption amount increased with both the concentration of methylene blue and the duration of exposure, with an optimal adsorption time of 120 min. These findings highlight the potential of microcrystalline cellulose to enhance the mechanical properties and adsorption performance of chitosan-based aerogels. They offer promising applications in water treatment and environmental remediation. Additionally, the Highest Occupied Molecular Orbital (HOMO) of chitosan spans both oxygen and nitrogen atoms, whereas in cellulose, the electron density is predominantly localized around oxygen atoms.

Keywords: Chitosan, cellulose, methylene blue, isotherm, kinetic

Introduction

Synthetic organic dyes are prevalent in various industries, including textiles, paper, plastics, and cosmetics, owing to their vibrant colors and chemical stability [1]. However, improper disposal of dye wastewater into rivers and other water bodies without adequate treatment poses severe environmental and ecological threats. Methylene Blue (MB) is a cationic dye known for its carcinogenic and toxic effects on human health [2]. It is water-soluble and forms

colored cations [3]. Recent advancements in dye removal technologies include various methods such as adsorption, oxidation, ion exchange, membrane separation, electrokinetic processes, and coagulation [4]. Among these techniques, adsorption is the most promising due to its high efficiency and stability [5].

Chitosan (CH) is the second most abundant natural polysaccharide after cellulose. Chitosan is derived from chitin through a deacetylation process, typically

¹Department of Chemical Sciences, Faculty of Science and Technology, Universiti Kebangsaan Malaysia, 43600, UKM Bangi, Selangor Darul Ehsan, Malaysia

²Water Analysis Research Center (ALIR), Faculty of Science and Technology, Universiti Kebangsaan Malaysia, 43600, Bangi, Selangor Darul Ehsan

³Polymer Research Center (PORCE), Faculty of Science and Technology, Universiti Kebangsaan Malaysia, 43600, Bangi, Selangor Darul Ehsan, Malaysia

⁴Department of Chemistry, Faculty of Science, Universiti Teknologi Malaysia, 81310, Skudai, Johor

⁵Advanced Functional Materials Research Group, Faculty of Industrial Technology, Institut Teknologi Bandung, Bandung 40132, Indonesia.

⁶Research Center for Nanosciences and Nanotechnology, Institut Teknologi Bandung, Bandung 40132, Indonesia

^{*}Corresponding author: nadhratunnaiim@ukm.edu.my

using highly concentrated sodium hydroxide as a reagent, as it does not occur naturally in its pristine form [6]. Although enzymatic processes are primarily limited to laboratory scales, the alkaline method is preferred in industry because of its efficiency, simplicity, and cost-effectiveness [7]. Chitosan is used in numerous fields, such as food, medicine, cosmetics, and wastewater treatment. Its valuable properties include its biocompatibility, nontoxicity, and biodegradability. The presence of active adsorption sites, such as amino (-NH₂) and hydroxyl (-OH) functional groups makes chitosan highly effective in dye adsorption processes [8].

Unfortunately, the application of chitosan in water treatment is hindered by its inherent limitations in terms of mechanical strength, stability, and solution separation capabilities [9]. Recent advancements have focused on enhancing the mechanical properties of chitosan-based adsorbents through chemical and physical modifications. Notably, the incorporation of cellulose has been extensively explored to improve the mechanical resilience of chitosan. This may be attributed to the formation of hydrogen bonds and excellent compatibility within the chitosan-cellulose, resulting in improved chemical and physical characteristics. Moreover, the integration of cellulose into chitosan matrices augments the availability of active sites for adsorbing dyes, such as methylene blue (MB) [10].

In this study, microcrystalline cellulose with a particle size of 20 µm has been employed, contrasting with the broader range (45.8 μm to 257 μm) utilized by Ozen et al. (2021). While their work concentrated on material preparation and characterization, it did not delve into dye adsorption properties [11]. In contrast, research specifically investigated microcrystalline cellulose affects the swelling properties and adsorption capacity of chitosanmicrocrystalline cellulose aerogels. We have systematically varied factors such dye concentration and contact time to optimize experimental conditions. Furthermore, the adsorption mechanism has been comprehensively examined using adsorption isotherms and kinetic models to elucidate the underlying processes governing dye uptake.

Materials and Methods Materials

Chitosan was purchased from Chito-Chem (M) Sdn. Bhd. Microcrystalline cellulose extracted from cotton linter (CAS: 9004-34-6) with 0.25 g/mL bulk density at 25°C and pH 5.0 - pH 7.0 was obtained from Sigma-Aldrich. The other reagents used were of analytical grade and used without further purification.

Preparation of chitosan-cellulose (CH-C) film aerogels

The experimental procedure for producing aerogels in this study was initiated by preparing a chitosancellulose solution mixture. Subsequently, the aerogels were freeze-dried at -40°C to -60°C for 48 h after direct freezing. Unlike conventional approaches where hydrogels are first formed and then dried, this method directly freezes the CH-C solution bypassing the hydrogel stage. For 48 h, 1 g of chitosan powder was dissolved in 50 mL of a 1% (v/v) acetic acid solution. Various concentrations of cellulose (C) were added in the CH solution: 0.125 g, 0.25 g, 0.5 g, 0.75 g, 1.0 g, and 1.5 g, respectively. To achieve a homogeneous solution, the CH-C mixture was stirred for 1 h and then sonicated for 30 min. After cooling for 48 h, CH-C aerogels were freeze-dried under vacuum. A pure CH aerogel film containing no cellulose used as a control was similarly prepared under identical conditions [12].

Swelling test

To determine the degree of swelling, each aerogel films was weighed and placed in deionized water for 24 h. The film was then removed from the medium and weighed after the removal of excess surface water using filter paper. The physical properties of pure chitosan film and reinforced chitosan film with cellulose were analyzed by measuring the thickness and length of the film as well as the swelling degree. The swelling degree was calculated using the Eq.(1) as follows [13-14]:

Swelling degree =
$$\frac{W_s - W_d}{W_d}$$
 (1)

where w_s is the swollen sample weight (g) and w_d is the dry sample weight (g).

Determination of pH_{pzc} value

The pH value at which the surface of the aerogel film carries no net charge is referred to as the point of zero charge (pH_{pzc}), which was determined using a solid addition method. In a beaker, 50 mL of NaCl (0.01 M) solution was prepared. To achieve the required acidic and alkaline pH levels, 0.1 M HCl or 0.1 M NaOH solutions were added to the 0.01 M NaCl solution. The aerogel films were then submerged in a prepared solution. The mixture was allowed to interact and stirred at 100 rpm using a magnetic stirrer. A pH meter was used to measure and record the final pH after removing the hydrogel film from the solution. The difference between the initial (pH_i) and final pH (pH_f) values was plotted against the pH_i. The pH where the ΔpH is equal to zero was referred to the pH_{pzc} of each aerogel [15].

Characterization of chitosan-cellulose aerogel

CH-C aerogel film was characterized using a Fourier transform infrared spectroscopy (FTIR) device from Perkin Elmer USA. The infrared spectrum was recorded in the frequency range of 4000-400 cm⁻¹. Infrared spectral analysis was performed to determine the functional groups on chitosan and cellulose. To confirm the crystallinity of the CH-C aerogel, X-ray diffraction analysis (D8-Advance, Bruker, Germany) was carried out using Cu K α radiation (α = 1.5418 nm) at 40 kV.

Effect of contact time on MB equilibrium adsorption

The effect of contact time on MB adsorption by the CH-C aerogel was investigated in a batch experiment, using 1 cm \times 1 cm of optimum CH-1.5 C aerogel and 20 mL of methylene blue (2 mg/L) at room temperature for a period ranging from 30 to 150 min. The batch adsorption experiments were performed in a conical flask and stirred with a magnetic stirrer at a speed of 100 rpm. The adsorbent was removed from the MB solution, while the remaining aqueous dye was analyzed using a UV-Vis spectrophotometer at 664 nm, which corresponds to the maximum capacity absorbency of methylene blue. The amount of adsorption at a time, q_t (mg/g) was calculated by Eq.(2) as follows [16]:

$$q_t = \frac{(c_o - c_t)}{W} V \tag{2}$$

where C_o is initial concentration of dye and C_t (mg/L) are the concentration of dye at time, V is the volume of solution (L) and W is the mass of dry adsorbent used (g).

Effect of concentration on MB equilibrium adsorption

For the quantity of MB adsorbed with various initial concentrations of MB at optimum contact time obtained, the adsorption capacity at equilibrium (dye adsorbed per unit quantity of sorbent), q_e was determined using Eq.(3) as follows [16]:

$$q_e = \left(\frac{c_o - c_e}{W}\right) V \tag{3}$$

here W = dry weight of the adsorbent (g), V = volume of dye solution (L), C_e = dye concentration at equilibrium.

Kinetic studies of adsorption

To examine the kinetic mechanism of the adsorption process of MB on the CH1.5 -C aerogel, pseudo-first-order and pseudo-second-order kinetic models were used. The pseudo-first-order rate equation of the

Lagergren model for the absorption of solid—liquid systems is as Eq.(4) [16]:

$$log (q_e - q_t) = log (q_e) - \frac{k_1}{2.303}t$$
 (4)

The pseudo-second-order rate equation is as Eq.(5) [16].

$$\frac{t}{q_t} = \frac{1}{k_2 q_{e^2}} - \frac{1}{q_e} \tag{5}$$

where q_e and q_t were the absorption capacity (mg/g) at equilibrium and at time t (min), respectively, k_1 (L min^{-1}) and k_2 (g (mg min)⁻¹) the absorption rate constants of pseudo-first order and pseudo-second-order absorption rates, respectively.

Isotherm studies of adsorption

Adsorption data were elicited using the Langmuir and Freundlich isotherm equations [16]. The Langmuir isotherm model estimates the maximum adsorption capacity corresponding to the complete monolayer coverage on the sample surface. The linear form of the Langmuir adsorption isotherm can be expressed as Eq.(6) follows:

$$\frac{C_e}{q_e} = \frac{1}{q_{max}K_L} + \frac{C_e}{q_{max}} \tag{6}$$

where K_L was constant of the sorption equilibrium (L/mg) and q_{max} was the maximum dye sorption capacity (mg/g). If the sorption is defined by Langmuir isotherm equation, plot of $\frac{1}{q_e}$ vs $\frac{1}{C_e}$ would be linear. The values of q_{max} and K_L can be obtained from the slope and intercept of the straight line.

The Freundlich adsorption isotherm model assumes that the adsorption occurs in a heterogeneous system. This model represents the balance between the amount of absorbent in the solution and the surface of the absorbent. This implies that adsorption occurs in the multilayer. The Freundlich isotherm equation is as Eq.(7) below:

$$\log q_e = \log K_F + \frac{1}{n} \ln C_e \tag{7}$$

where K_F and n are adsorption constants for measuring adsorption capacity, 1/n is intensity of adsorption. 1/n value represents adsorption process to be unfavorable (1/n > 2) or favorable (0.1 < 1/n < 0.5). The slope 1/n, ranging from 0 to 1, measures the surface heterogeneity, and values closer to zero indicate high heterogeneity.

Computational method

Density functional theory (DFT) calculations to determine electronic properties were conducted using the Gaussian 09 software. HOMO and LUMO were defined as Highest Occupied Molecular Orbital and Lowest Unoccupied Molecular Orbital, respectively. The BLYP/6-311+G(d) basis set was used in this study. To enhance computational efficiency, only the monomeric units of chitosan and cellulose were modelled. It was assumed that the molecular interactions between cellulose and chitosan were qualitatively like those between the chitosan polymer chains and cellulose. The reactivity of organic molecules is characterized by their electrophilicity index (ω), electronic chemical potential (μ), chemical hardness (η) , and softness (S). These parameters were derived from the one-electron energies of the HOMO and LUMO frontier molecular orbitals (FMO), which are expressed at Eq. (8) as follows:

$$\omega = \frac{\mu^2}{2\eta}$$

$$\mu = \frac{E_H + E_L}{2}$$

$$\eta = E_L - E_H$$

$$S = \frac{1}{\eta}$$
(8)

where E_H and E_L are the HOMO and LUMO energy levels energies, respectively.

Results and Discussion

Fourier Transform Infrared Spectroscopy (FTIR)

The FTIR spectra presented in **Figure 1** illustrates the characteristics of chitosan powder and the aerogel film derived from chitosan-cellulose. The peaks at 3350 cm⁻¹ and 3285 cm⁻¹ are attributed to N-H and O-H stretching, respectively, while the absorption bands at approximately 2925 cm⁻¹ and 2869 cm⁻¹ correspond to C-H symmetric and asymmetric stretching, respectively. The bands at 1627 cm⁻¹ and 1575 cm⁻¹ signify C=O stretching and NH bending of the amide II, respectively. The presence of ether (C-O-C) and carbonyl (C-O) functional groups in chitosan is confirmed by the peaks observed at 1077 cm⁻¹ and 1023 cm⁻¹ [17-18]. Additionally, the absorption peak at 888 cm⁻¹ indicates the presence of a β -(1,4)-glycosidic bond in chitosan.

Notably, no new peaks emerged in the spectra of the chitosan-cellulose aerogel, suggesting that cellulose was incorporated into the chitosan molecules without forming new covalent bonds. Instead, a noticeable shift occurred at the existing peaks. Specifically, the shifts in the absorption peaks of –OH and –NH₂ from 3350 cm⁻¹ and 3285 cm⁻¹ to 3372 cm⁻¹ and 3108 cm⁻¹, respectively, suggest the formation of strong hydrogen bonds between chitosan and cellulose. The shift in the peaks indicates cellulose interaction and integration into the chitosan matrix while forming the aerogel.

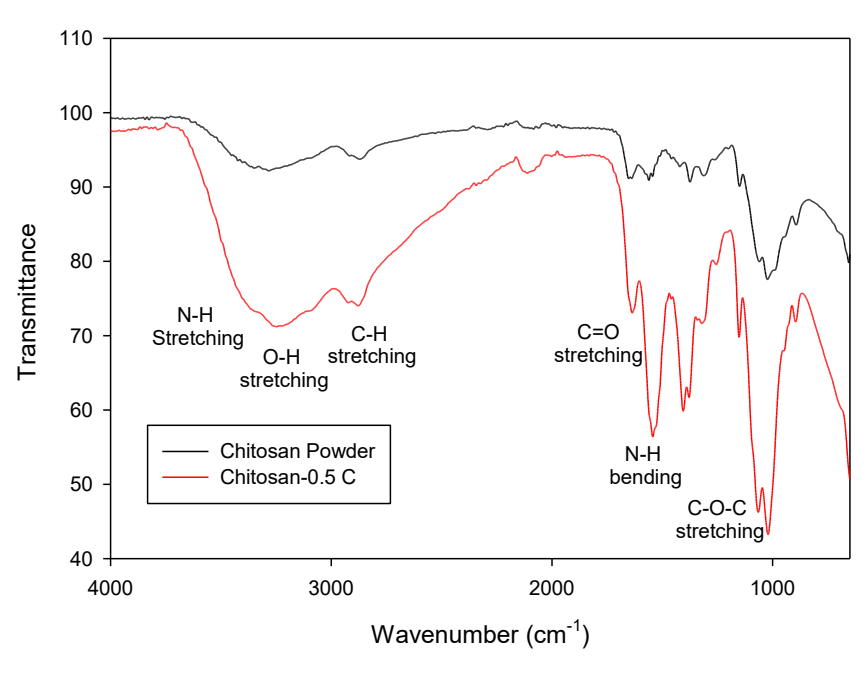
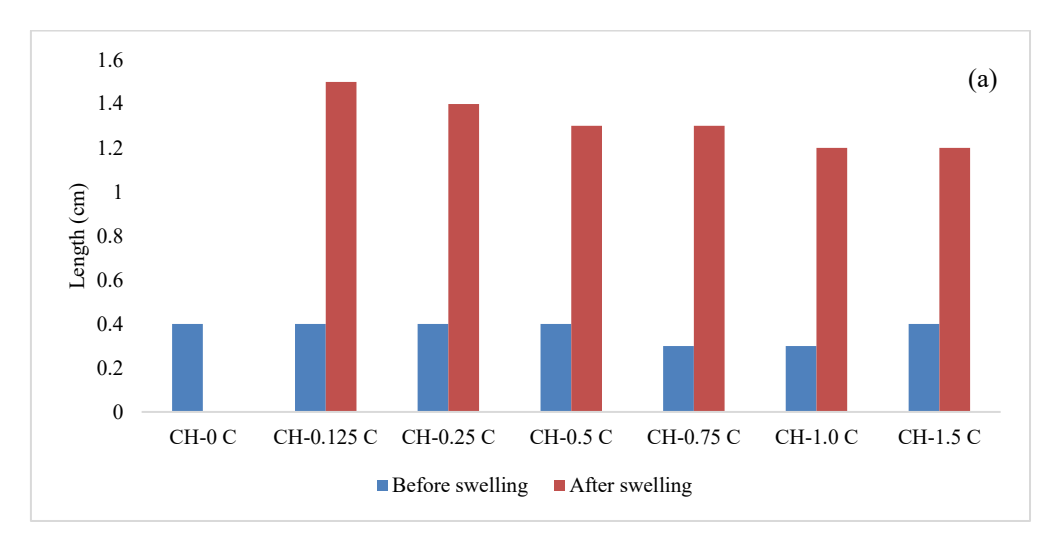


Figure 1. FTIR spectra for Chitosan powder and chitosan-cellulose aerogel

Swelling test

Figures 2(a) and 2(b) show the conditions of the aerogel film before and after a 24-hour swelling duration. Notably, CH-0 C underwent complete degradation in DI water after immersion in distilled water. Conversely, the addition of cellulose to the chitosan aerogel film significantly enhanced its ability to retain its shape. The CH-1.5 C aerogel, which had the highest cellulose content, remained intact even after 24 h of immersion in deionized water. This supports the conclusion that the addition of cellulose strengthens the structure of an aerogel based on chitosan [19]. The inclusion of cellulose results in the formation of a strong hydrogen bond with the functional group present in the chitosan structure [20].

It can also be observed that the elongation and thickness of the aerogel decreased as the cellulose content increased. This indicates a reduction in water uptake owing to the presence of strong hydrogen bonds between cellulose and chitosan. Figure 3 also demonstrates a decrease in the swelling degree from CH-0.125 C to CH-1.5 C aerogel films as more cellulose was integrated into the chitosan aerogels. The swelling decreased from 32.30 g/g (CH-0.125 C) to 17.93 g/g (CH-1.5 C), indicating a negative correlation between cellulose loading and water uptake. This is due to increased crystallinity and hydrogen bonding which reduce pore accessibility. This trend aligns with the findings of Chang et al. (2010), suggesting that the bonds within the aerogel structure influence the degree of swelling, with an increase in hydrogen bonds observed in CH-C aerogels as the cellulose weight increases [21].



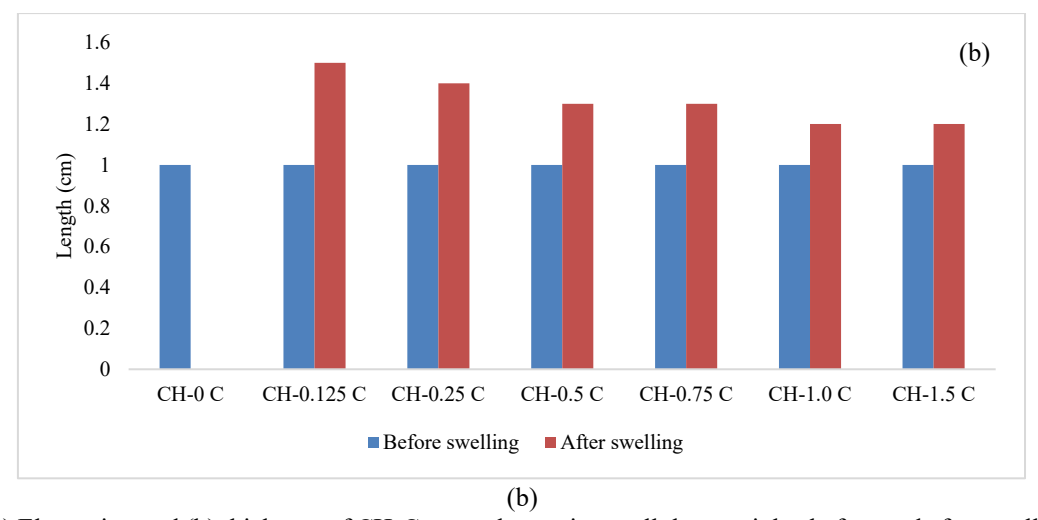


Figure 2. (a) Elongation and (b) thickness of CH-C aerogel at various cellulose weights before and after swelling

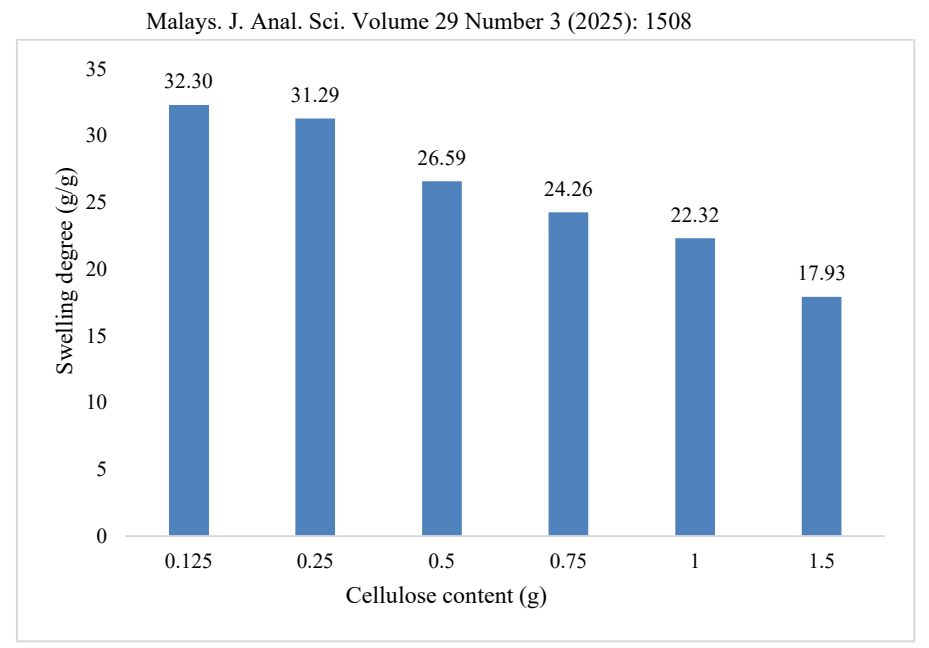


Figure 3. Swelling degree of CH-C aerogels film

Determination of pH_{pzc} value

Figure 4 shows the point of zero charge (pH_{pzc}) value for all CH-C aerogel films. The incorporation of different cellulose weights does not significantly effect the pH_{pzc} value. Specifically, the pH_{pzc} values for all aerogels, are in the range of 5.2-5.3. It can also be observed that at pH values $< pH_{pzc}$, the surface of the aerogel film is positively charged because the pH changes to a lower pH. This is because the $-NH_2$ group is protonated and becomes a NH_3^+ ion. However, the surface of the film is negatively charged at pH $> pH_{pzc}$ because the -OH group becomes O^-

ion. Therefore, the adsorption of methylene blue could occur at $pH > pH_{pzc}$ (5.18 to 5.35) because it will lead to the adsorption of the cationic dye MB through electrostatic attraction with the negatively charged chitosan-cellulose-based aerogel film surface [22]. Therefore, in this study, the pH of the methylene blue solution used was 7. Both neutral and alkaline solutions benefit the adsorption process because the availability of anionic sites on the surface of the adsorbent is significantly higher than that of the adsorbent.

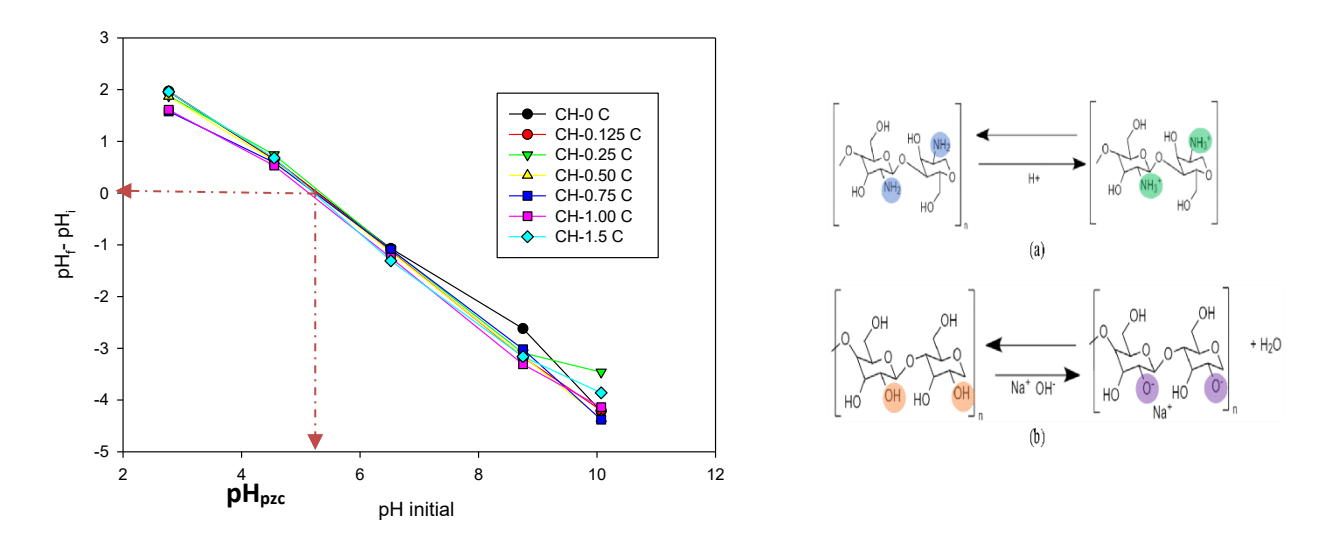
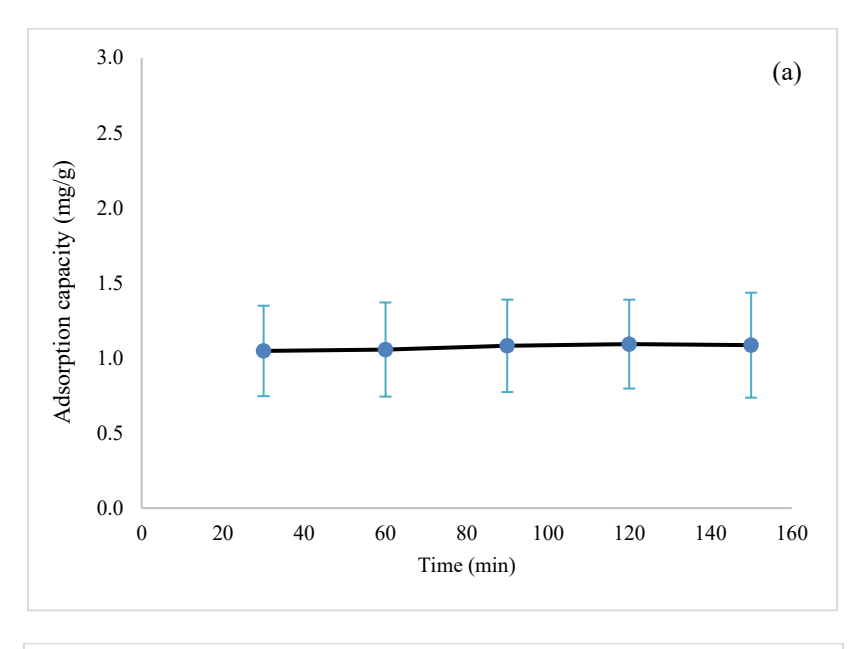


Figure 4. pH_{pzc} point for chitosan-cellulose aerogel

Sorption study towards methylene blue

Figures 5 (a) and **(b)** show the effect of time and initial concentration on the removal of methylene blue by the CH-1.5 C aerogel, respectively. It can be observed that after 30 minutes, the sorption capacity of CH-1.5 C aerogel slightly increased from 1.04 mg/g to 1.09 mg/g. However, after 120 min, the sorption capacity decreased slightly over time. This phenomenon is due to the adsorption process. During the early stages of contact, the adsorption sites on the CH-1.5 C aerogel are unoccupied, allowing methylene blue (MB) ions to readily bind to them [23]. Consequently, the sorption capacity increases as more dye molecules are adsorbed. However, as the contact time increased, the available vacancies on the sorbent

surface diminished continuously [24]. It becomes increasingly challenging for additional MB ions to occupy the active sorption sites owing to the reduced availability of vacant sites. As a result, excess dye molecules were not adsorbed on the binding site, thus reducing the sorption capacity [25]. Meanwhile for the effect of initial concentration, the adsorption capacity of CH-1.5 C aerogel increased from 0.17 mg/g to 0.39 mg/g with the increasing initial concentration of MB from 2 ppm to 4 ppm. However, it is notable that there is competition for available sites, as well as a decrease in adsorption capacity. Complete binding of the sorption sites with MB molecules occurs when the maximum sorption capacity of the adsorbent is reached [26].



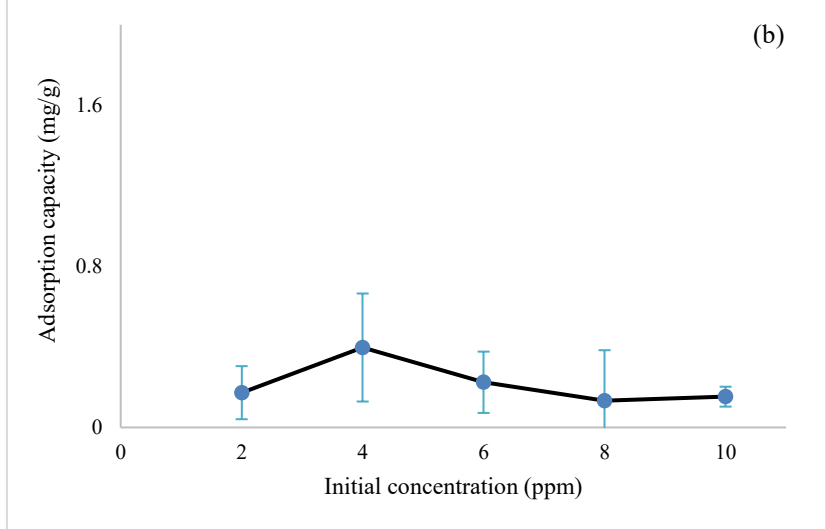


Figure 5. Adsorption of methylene blue by aerogel CH-1.5 C as a (a) function of time and (b) initial concentration

Overall, Table 1 shows that the R² value for the second-order model is higher than that for the firstorder model. Besides that, the second-order pseudo q_e value which is 1.093 mg/g is closer to the experimental q_e value of 1.092 mg/g compared to the first-order pseudo q_e value of 0.234 mg/g. The higher value of R^2 (0.9998) and close to the experimental q_e value proves that this data is suitable for the secondorder pseudo model. Therefore, it can be said that the absorption of methylene blue conforms to the secondorder pseudo-model, where the absorption mechanism is dependent on chitosan-cellulose-based aerogel and methylene blue [27]. Furthermore, Table 2 shows that the R² value for the Langmuir isotherm model is 0.9177, which is higher than that of the Freundlich isotherm model. This indicates that MB adsorption occurred on the surface of the chitosan-cellulosebased aerogel.

Interaction studies

DFT calculations were performed to investigate the interactions between chitosan and cellulose. As shown in Figure 6, the Highest Occupied Molecular Orbital (HOMO) of chitosan spans both oxygen and nitrogen atoms, whereas in cellulose, the electron density is predominantly localized around oxygen atoms. Moreover, the energy gap between the HOMO and LUMO levels was found to be narrower for chitosan $(\eta = 6.48 \text{ eV})$ than for cellulose $(\eta = 7.47 \text{ eV})$, indicating the slightly higher reactivity of chitosan. Additionally, the quantum chemical descriptor in Fig. 6 reveals that the electrophilicity of chitosan surpasses those of cellulose, suggesting a greater degree of electrophilicity in chitosan [28]. Overall, it can be seen from optimized structures of chitosan and cellulose illustrated in Figure 7, O, OH, and NH₂ groups carry negative charges. The hydrogen atoms within chitosan and cellulose can engage in hydrogen bonding with these groups.

Table 1. Pseudo-first and pseudo-second-order kinetic constants based on methylene blue absorption

Experimental	Pseudo-First-Order Constants			Pseudo-Second-Order Constants		
q (mg/g)	q e	(k ₁) k ₁	\mathbb{R}^2	qe	$\frac{(k_2)}{\mathbf{k}_2}$	\mathbb{R}^2
	(mg/g)	(1/min)		(mg/g)	(g(m.min))	
1.092	0.234	1.583x 10 ⁻⁵	0.784	1.093	1.033	0.9998

Table 2. The Langmuir and Freundlich isotherms model constants for the sorption of methylene blue by CH-C

		Langmı	ıir	Freundlich			
Aerogel	L	mg	\mathbf{R}_{L}	R^2	L 1/n R^2		
	$K_L(\frac{mg}{mg})$	$q_{max}(g)$			$K_F(\overline{mg})$		
CH-1.5 C	39.03	0.0959	0.0043	0.9177	3.474 0.916 0.1573		

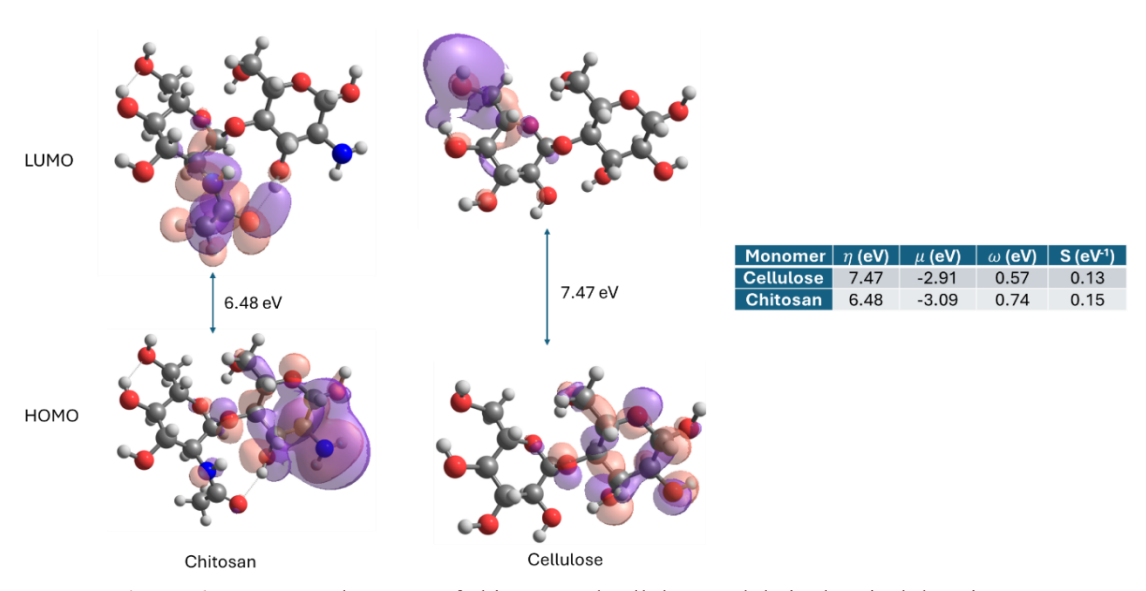
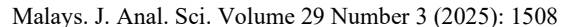


Figure 6. HOMO and LUMO of chitosan and cellulose and their chemical descriptors



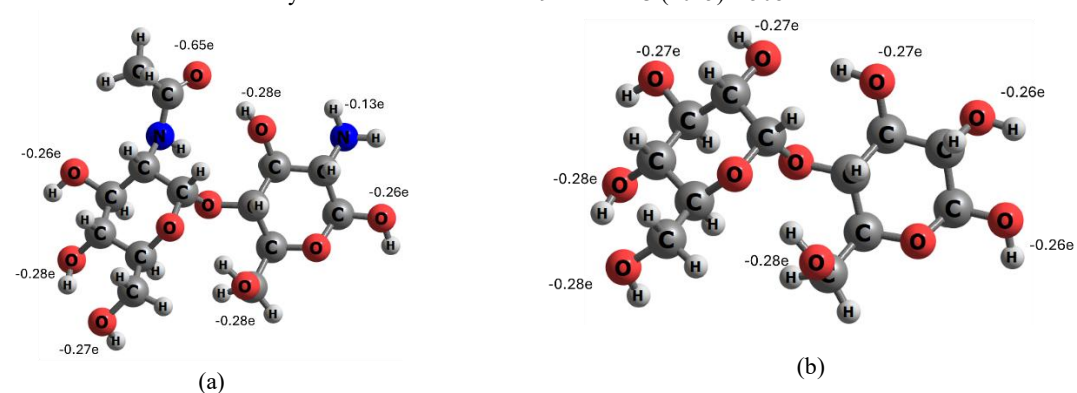


Figure 7. Optimized structure of (a) chitosan and (b) cellulose monomers. The numbers represent the natural charge of the groups of interest

We also analyzed the hydrogen bond interactions that occur between the OH, O, and NH₂ groups of chitosan and cellulose when they come into contact. Based on the optimized geometries for these interactions, as shown in **Figure 8**, the structures demonstrated similar interaction energies, indicating that they have comparable probabilities of forming when chitosan and cellulose come into contact, irrespective of the electronegativity of the atoms involved.

We also investigated the interaction of chitosancellulose with a methylene blue (MB) molecule. Our results, as illustrated in **Figure 9**, demonstrate that the MB molecule can effectively bind to the chitosancellulose. In all configurations, the NH group of the MB molecule forms a stable hydrogen bond with the oxygen atom of the OH groups in the chitosan-cellulose. Both the chitosan and cellulose components can interact with the MB molecule, exhibiting appropriate interaction energies. However, it is also observed that several functional groups in cellulose exhibit stronger interactions compared to chitosan. This difference may be attributed to the greater electrophilicity of chitosan compared to cellulose. These findings align with experimental data which indicates that the presence of cellulose in the chitosan structure not only aids in retaining the shape of chitosan aerogel in water but also enhances the absorption capacity of methylene blue.

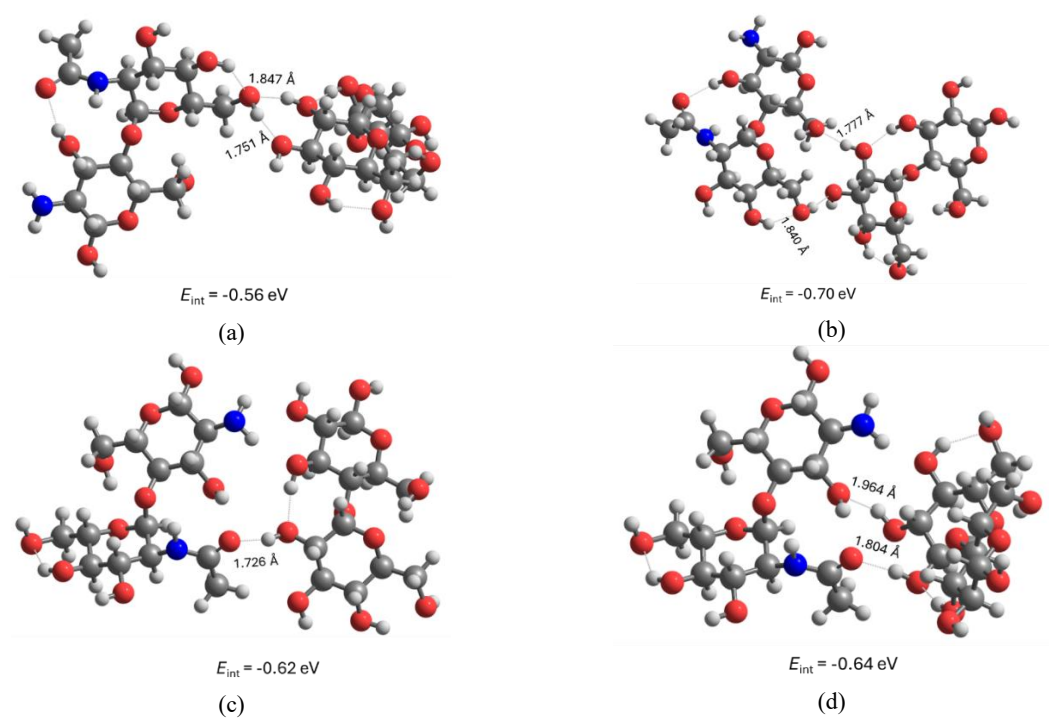


Figure 8. Optimized structure of chitosan-cellulose interactions. (a) OH group at C6 of N-acetylglucosamine rings, (b) hydroxyl group at C6 of glucosamine rings, (c) C=O group at N-acetylglucosamine rings, and (d) OH group at C3 of glucosamine rings

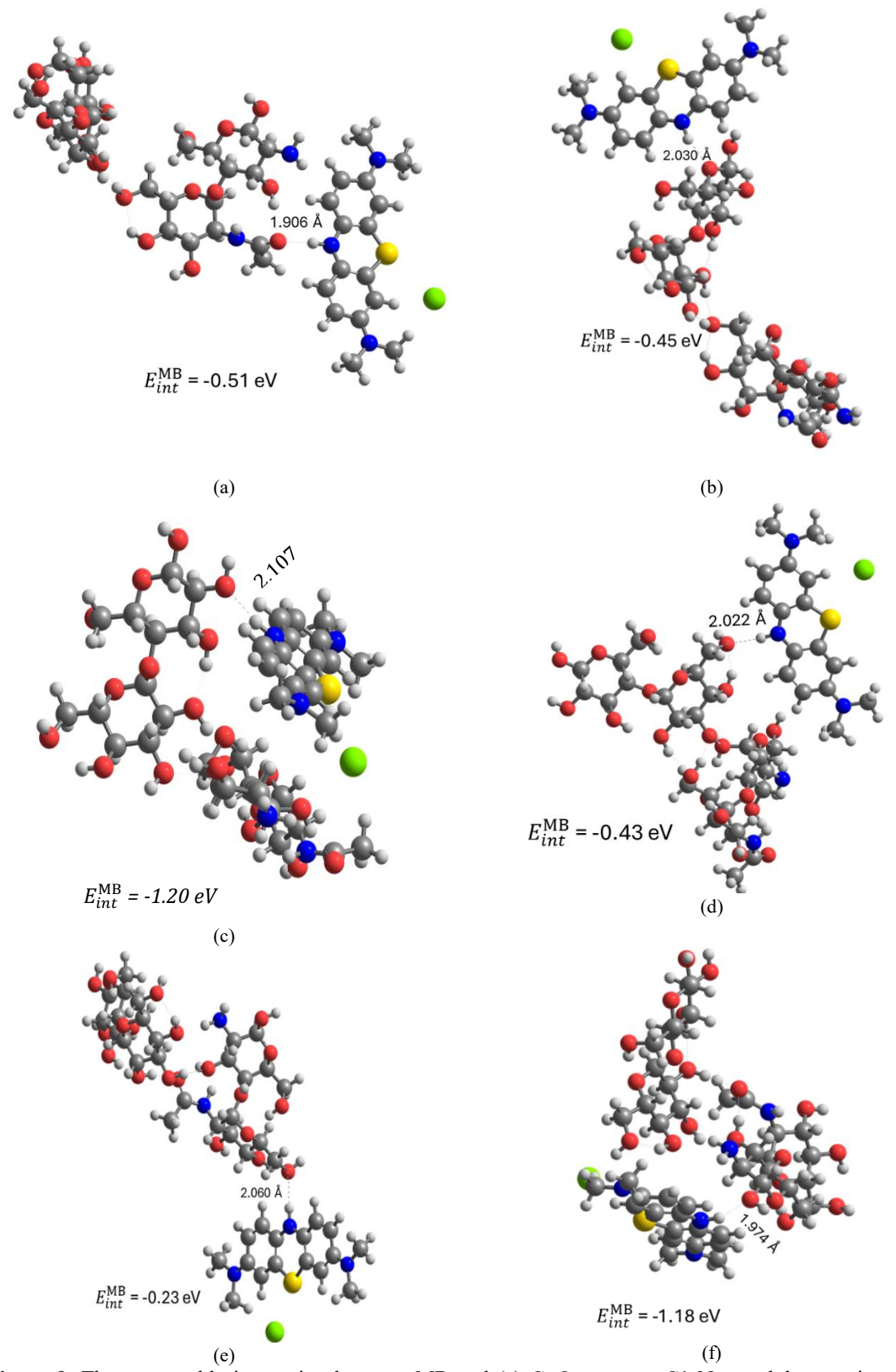


Figure 9. The most stable interaction between MB and (a) C=O group at C1 N-acetylglucosamine rings of chitosan, (b) C-O-C group at cellulose, (c) OH group at C2 of cellulose, (d) OH group at C1 of cellulose, (e) OH group at C6 glucosamine rings of chitosan and (f) OH group at C1 glucosamine rings of chitosan

Conclusion

This study demonstrates that the incorporation of cellulose into chitosan-based microcrystalline aerogels significantly enhances their structural retention stability. The adsorption behavior of methylene blue (MB) followed the Langmuir isotherm model, indicating monolayer adsorption on a homogeneous surface. Kinetic analysis revealed that the adsorption process fits the pseudo-second-order model, suggesting that physical adsorption dominates the interaction between the dye molecules and the aerogel surface. Besides that, spectroscopic analysis confirmed physical interactions between chitosan and cellulose, while computational studies indicated that hydrogen atoms within both polymers are capable of forming hydrogen bonds with electronegative groups such as O, OH, and NH₂, due to their negative charges. The interaction energies suggest that electronegative atoms in chitosan and cellulose have comparable probabilities of forming hydrogen bonds when in contact. Additionally, the NH group of the MB molecule forms stable hydrogen bonds with the OH groups of the chitosan-cellulose matrix. Both chitosan and cellulose contribute to the adsorption process. However, several functional groups in cellulose exhibit stronger interactions with MB compared to this chitosan. Overall, study shows microcrystalline cellulose not only enhances the structural stability of chitosan aerogels but also actively contributes to their interaction methylene blue during the adsorption process.

Acknowledgement

This research is financially supported by Ministry of Higher Education through Fundamental Research Grant Scheme [FRGS/1/2024/STG04/UKM/02/5]. The authors would also like to express their gratitude to the Faculty of Science and Technology (FST) at the Universiti Kebangsaan Malaysia (UKM) for their technical support and facilities provided. Additionally, we acknowledge the support provided by ITB through the "Riset International 2023" program for the interaction studies conducted using DFT.

References

- Filipkowska, U., Klimiuk, E., Grabowski, S., and Siedlecka, E. (2002). Adsorption of reactive dyes by modified chitin from aqueous solutions. *Polish Journal of Environmental Studies*, 11(4): 315-324.
- 2. Manning, B. W., Cerniglia, C. E., and Federle, T. W. (1985). Metabolism of the benzidine-based azo dye direct black 38 by human intestinal microbiota. *Applied and Environmental Microbiology*, 50(1): 10-15.
- 3. Nony, C. R., and Bowman, M. C. (1980). Trace analysis of potentially carcinogenic metabolites

- of an azo dye and pigment in hamster and human urine as determined by two chromatographic procedures. *Journal of Chromatographic Science*, 18(2): 64-74.
- Salleh, M. A. M., Mahmoud, D. K., Karim, W. A. W. A., and Idris, A. (2011). Cationic and anionic dye adsorption by agricultural solid wastes: *A comprehensive review. In Desalination*, 280: 1–3.
- 5. Kyzas, G. Z., Fu, J., and Matis, K. A. (2013). The change from past to future for adsorbent materials in treatment of dyeing wastewaters. *Materials*, 6(11): 5131-5158.
- Novikov, V. Y., Derkach, S. R., Konovalova, I. N., Dolgopyatova, N. V, and Kuchina, Y. A. (2023). Mechanism of heterogeneous alkaline deacetylation of chitin: A review. *Polymers*, 15(7).
- Hamed, I., Özogul, F., and Regenstein, J. M. (2016). Industrial applications of crustacean byproducts (chitin, chitosan, and chitooligosaccharides): A review. *Trends in Food Science & Technology*, 48: 40-50.
- Jawad, A. H., Azharul Islam, M., and Hameed, B. H. (2017). Cross-linked chitosan thin film coated onto glass plate as an effective adsorbent for adsorption of reactive Orange 16. *International Journal of Biological Macromolecules*, 95: 743-749.
- Nawi, M. A., Jawad, A. H., Sabar, S., and Ngah, W. S. W. (2011). Photocatalytic-oxidation of solid state chitosan by immobilized bilayer assembly of tio2-chitosan under a compact household fluorescent lamp irradiation. Carbohydrate Polymers, 83(3): 1146-1152.
- Pang, Y. L., Tan, J. H., Lim, S., and Chong, W. C. (2021). A state-of-the-art review on biowaste derived chitosan biomaterials for biosorption of organic dyes: Parameter studies, kinetics, isotherms and thermodynamics. *Polymers*, 13(17): 3009.
- 11. Ozen, E., Yildirim, N., Dalkilic, B., and Ergun, M. E. (2021). Effects of microcrystalline cellulose on some performance properties of chitosan aerogels. *Maderas. Ciencia y tecnología*, 23: 26.
- 12. Yang, H., Sheikhi, A., and Van De Ven, T. G. M. (2016). Reusable green aerogels from crosslinked hairy nanocrystalline cellulose and modified chitosan for dye removal. *Langmuir*, 32(45): 11771-11779.
- Hakam, A., Rahman, I. A., Jamil, M. S. M., Othaman, R., Amin, M. C. I. M., and Lazim, A. M. (2015). Removal of methylene blue dye in aqueous solution by sorption on a bacterial-gpoly-(acrylic acid) polymer network hydrogel. *Sains Malaysiana*, 44(6): 827-834.
- 14. Huo, M. X., Jin, Y. L., Sun, Z. F., Ren, F., Pei, L., and Ren, P. G. (2021). Facile synthesis of

- chitosan-based acid-resistant composite films for efficient selective adsorption properties towards anionic dyes. *Carbohydrate Polymers*, 254(11): 117473.
- 15. Ntakirutimana, S., Tan, W., and Wang, Y. (2019). Enhanced surface activity of activated carbon by surfactants synergism. *RSC Advances*, *9*(45): 26519-26531.
- 16. Shetty, B. (2022). A Green approach to the removal of malachite green dye from aqueous medium using chitosan/cellulose blend: pp. 1-26.
- 17. Li, Q., Zhou, J., and Zhang, L. (2009). Structure and properties of the nanocomposite films of chitosan reinforced with cellulose whiskers. Journal of polymer science part B: Polymer physics, 47(11): 1069-1077.
- Yasmeen, S., Kabiraz, M. K., Saha, B., Qadir, M. D., Gafur, M. D., and Masum, S. (2016). Chromium (VI) ions removal from tannery effluent using chitosan-microcrystalline cellulose composite as adsorbent. *International Research Journal Pure Applied Chemistry*, 10(4): 1-14.
- 19. Mao, H., Wei, C., Gong, Y., Wang, S., and Ding, W. (2019). Mechanical and water-resistant properties of eco-friendly chitosan membrane reinforced with cellulose nanocrystals. *Polymers*, 11(1): 166.
- Huang, X., Xie, F., and Xiong, X. (2018). Surface-modified microcrystalline cellulose for reinforcement of chitosan film. *Carbohydrate Polymers*, 201: 367-373.
- 21. Chang, P. R., Jian, R., Yu, J., and Ma, X. (2010). Fabrication and characterisation of chitosan nanoparticles/plasticised-starch composites. *Food Chemistry*, 120(3): 736-740.
- 22. Khademian, E., Salehi, E., Sanaeepur, H., Galiano, F., and Figoli, A. (2020). A systematic review on carbohydrate biopolymers for

- adsorptive remediation of copper ions from aqueous environments-part A: Classification and modification strategies. *Science of the Total Environment*, 738: 139829.
- Wang, J., Wang, L., Yu, H., Zain-ul-Abdin, Chen, Y., Chen, Q., Zhou, W., Zhang, H., and Chen, X. (2016). Recent progress on synthesis, property and application of modified chitosan: An overview. *International Journal of Biological Macromolecules*, 88: 333-344.
- 24. Muinde, V. M., Onyari, J. M., Wamalwa, B., and Wabomba, J. N. (2020). Adsorption of malachite green dye from aqueous solutions using mesoporous chitosan–zinc oxide composite material. *Environmental Chemistry and Ecotoxicology*, 2: 115-125.
- 25. Rangabhashiyam, S., Anu, N., and Selvaraju, N. (2013). Sequestration of dye from textile industry wastewater using agricultural waste products as adsorbents. *Journal of Environmental Chemical Engineering*, 1(4): 629-641.
- 26. Sun, X. F., Liu, B., Jing, Z., and Wang, H. (2015). Preparation and adsorption property of xylan/poly(acrylic acid) magnetic nanocomposite hydrogel adsorbent. *Carbohydrate Polymers*, 118: 16-23.
- Meroufel, B., Benali, O., Benyahia, M., Benmoussa, Y., and Zenasni, M. A. (2013). Adsorptive removal of anionic dye from aqueous solutions by Algerian kaolin: Characteristics, isotherm, kinetic and thermodynamic studies. *Journal of Materials and Environmental Science*, 4(3): 482-491.
- 28. Dhananasekaran, S., Palanivel, R., & Pappu, S. (2016). Adsorption of methylene blue, bromophenol blue, and coomassie brilliant blue by α-chitin nanoparticles. *Journal of Advanced Research*, 7(1): 113-124.